Journal of Zhejiang University-SCIENCE A (Applied Physics & Engineering)
ISSN 1673-565X (Print); ISSN 1862-1775 (Online)
www.zju.edu.cn/jzus; www.springerlink.com
E-mail: jzus@zju.edu.cn

Relationship between chloride diffusivity and pore structure of hardened cement paste*

Guo-wen SUN†, Wei SUN†‡, Yun-sheng ZHANG, Zhi-yong LIU

(*Jiangsu Key Laboratory of Construction Materials, Southeast University, Nanjing 211189, China*)

†E-mail: sunguowen_2003@163.com; sunwei@seu.edu.cn

Received Sept. 18, 2010; Revision accepted Jan. 16, 2011; Crosschecked Apr. 20, 2011

Abstract: Based on effective media theory, a predictive model, relating chloride diffusivity to the capillary pores, gel pores, tortuosity factor, and pore size distribution of hardened cement, is proposed. To verify the proposed model, the diffusion coefficient of chloride ions, the degree of hydration, and peak radius of capillary pores of cement paste specimens were measured. The predicted results for chloride diffusivity were compared with published data. The results showed that the predicted chloride diffusivity of hardened cement paste was in good agreement with the experimental results. The effect of the evolution of pore structures in cement paste on chloride diffusivity could be deduced simultaneously using the proposed model.

Key words: Hardened cement paste, Chloride diffusivity, Porosity, Tortuosity factor, Constrictivity
doi:10.1631/jzus.A1000413 **Document code:** A **CLC number:** TU528

1 Introduction

In the service environment, owing to the porous nature of concrete, chloride ions penetrate concrete and induce the corrosion of embedded reinforcing steel, leading to premature deterioration of the concrete structure. The extent of steel corrosion depends largely on the chloride ion diffusion coefficients in hardened cement paste (Mindess *et al.*, 2002; Zhang and Ba, 2010). Thus, it is especially important to determine the diffusion coefficient of chloride ions to predict the time of initiation of corrosion and estimate the durability of a concrete structure. It is essential to establish a quantitative relationship between chloride diffusivity and the microstructure of the cement paste, such as the evolution of its pore structure. Only if that the relationship between chloride diffusivity and the evolution of pore structure is determined can the chloride ion transport behavior be defined and the durability of concrete be accurately evaluated.

Until now, researchers have focused mainly on building the relation between chloride diffusivity and the porosity of cement paste. Halamickova *et al.* (1995) quantitatively related the chloride diffusion coefficient to the critical pore diameter of capillary pores of cement paste. Pivonka *et al.* (2004) determined the relation between the chloride diffusion coefficient and the porosity and pore solution of cement paste. Huang *et al.* (2010) investigated the relation between chloride diffusivity and the pore solution of cement, based on the generalized effective medium theory. Zhang *et al.* (2010) researched the effect of the porosity of fresh concrete on chloride diffusion coefficients. However, the transport behavior of chloride ions in cement relates not only to total porosity and the concentration of the pore solution, but also to other pore structure parameters such as porosity, connectivity, size distribution, tortuosity, and the interaction between pore structure and transport ions. Of

‡ Corresponding author

* Project supported by the National Basic Research Program (973) of China (No. 2009CB623200), the National High-Tech R&D Program (863) of China (No. 2008AA030794), and the Postgraduates Research Innovation in University of Jiangsu Province, China (No. CX10B-064Z)

course, for concrete structures exposed long term to sea water and/or deicing salt, the binding capacity of chloride ions also has a significant effect on the chloride diffusion process. Ishida *et al.* (2009) proposed a chloride transport model considering chloride ion binding capacity and the constrictivity factor. In addition, Ishida *et al.* (2008) have established the quantitative relationship between chloride ion binding capacity and different types of admixtures, and the replacement ratio. We did not consider the binding capacity of chloride ions in our research because we determined the diffusion coefficient using a rapid accelerated migration test. As a rule, the diffusion coefficient is determined by experiment for each specimen. Due to experimental error, different researchers always obtain different results, even if the raw materials are identical. It is increasingly recognized that a reliable predictive model of chloride diffusivity is urgently needed.

The aim of this research was to develop a reliable predictive model based on the relationship between chloride diffusivity and the evolution of pore structure, to deduce the chloride ion transport behavior of hardened cement paste.

2 Microstructure of the hardened cement paste

Hardened cement paste is composed of unhydrated cement particles, hydration products, water, a small amount of air, and pore networks occupied by the bulk water and air at normal temperature. It is regarded as a two-phase composite, with a pore phase and a solid phase, consisting of various hydration products, in a saturated state (Fig. 1a). The pore network of cement paste comprises interlayer porosity, gel pores, capillary pores, and macropores, which forms transport pathways of aggressive medium intruded in the hardened cement paste. Maekawa *et al.* (2003) considered that no ions are transported into the interlayer pores of cement paste since the molecular-related size of the interlayer space is too small to accommodate them. Therefore, the three types of pores are taken into account in this study. A schematic diagram of the structural model of pores of hardened cement paste is depicted in Fig. 1b.

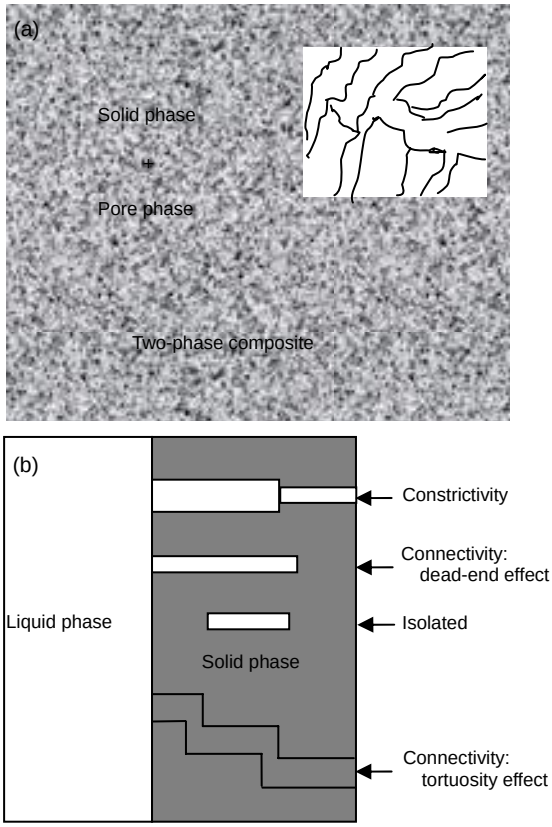

Fig. 1 Component (a) and pore structure (b) of hardened cement paste

Note that the calcium silicate hydrates (C-S-H) gel pores are included in the solid phase, not in the pore phase. The main path of transport in hardened cement paste is known to be the capillary pore space while the gel pores play a minor role (Garboczi and Bentz, 1992), except at very low capillary porosity. During the initial stages of cement hydration, the transport properties of cement paste are very good since all of the pores are fully connected. However, as hydration increases, hydration products grow into the pore spaces. Consequently, the pores become smaller and only partially connected, so that the transport properties of the cement paste decrease.

The pores in hardened cement paste can be classed as either continuous (including those with a tortuosity effect), continuous with an ink-bottle shape, dead-end with an ink-bottle shape, or isolated pores (Fig. 1b). Continuous pores, also called effective pores, play an important role in transport pathways in aggressive media. Dead-end pores and

isolated pores do not contribute to transport properties. Usually, a tortuous continuous pore can be expressed by the parameter of tortuosity or the tortuosity factor, while a continuous pore with an ink-bottle shape can be described by the constrictivity of the pore network, since the constrictivity takes into account the interaction between pore structure and ion transport (Maekawa *et al*., 2003).

3 Effective media theory

The effective diffusivity of a porous material can be expressed by the relationship between pore structure parameters (Oh and Jang, 2004):

$$\frac{D_\mathrm{p}}{D_0}=\phi_\mathrm{cap}\frac{\delta}{\tau^2}, \tag{1}$$

where D_p is the effective diffusivity of a porous material (m^2/s), ϕ_cap is the capillary porosity, and τ and δ are the tortuosity factor and constrictivity of the pore network, respectively; D_0 is the diffusivity of ions transported in bulk water, i.e., $D_0=2.03\times10^{-9}$ m^2/s for chloride ions at 25 °C.

However, the solid phase of the cement paste also has pores, i.e., C-S-H gel pores, and is also diffusive (Garboczi and Bentz, 1992). So, a formula more appropriate than Eq. (1) is proposed:

$$\frac{D_\mathrm{p}}{D_0}=V_\mathrm{T-por}\frac{\delta}{\tau^2}, \tag{2}$$

$$V_\mathrm{T-por}=V_\mathrm{cap}+V_\mathrm{gel}, \tag{3}$$

where $V_\mathrm{T-por}$ is the total porosity; V_cap and V_gel are the porosities of capillary and gel pores, respectively, and can be calculated for Portland cement as follows:

$$V_\mathrm{gel}=\frac{0.19\alpha}{w/c+0.32}, \tag{4}$$

$$V_\mathrm{cap}=\frac{w/c-0.36\alpha}{w/c+0.32}, \tag{5}$$

where w/c is the ratio of water to cement, and α is the degree of hydration.

So the total porosity can be obtained by substituting Eqs. (4) and (5) into Eq. (3):

$$V_\mathrm{T-por}=\frac{w/c-0.17\alpha}{w/c+0.32}, \tag{6}$$

which illustrates that the development of porosities can be determined when w/c and α are known.

A continuous pore with a tortuous character can be represented by the parameter of tortuosity:

$$\zeta=l_\mathrm{e}/l, \tag{7}$$

where l_e is the ratio of the length of the actual ion transport pathways, and l is the corresponding length in the projected plane (Fig. 2).

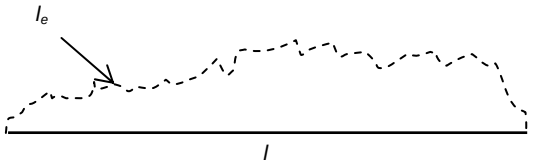

Fig. 2 Definition of tortuosity

Tortuosity is an intrinsic characteristic expressing the geometrical property of pore structure, and can be assumed to be independent of the characteristics of ions. In fact, it is very difficult to measure the tortuosity (ζ) of the pore network in hardened cement paste, so it is calculated using the material's permeability (AutoPore IV 9500, 2001):

$$\zeta=\sqrt{\frac{D_\mathrm{avg}^2}{4.24K(1+\rho_\mathrm{s}V_\mathrm{tot})}}, \tag{8}$$

where K and V_tot are the permeability (m/s) and total volume of the porous material (m^3/kg), respectively. ρ_s and D_avg^2 can be obtained by mercury intrusion porosimetry (MIP) measurements, where ρ_s is the apparent density of the material (kg/m^3), and D_avg is the weighted average of the pore diameter (m):

$$D_\mathrm{avg}^2=\rho_s\left[\frac{1}{2}I_1D_1^2+\sum_{i=2}^{n-1}I_iD_i^2+\frac{1}{2}I_nD_n^2\right], \tag{9}$$

where I_i and D_i are the specific intrusion volume and pore diameter for the ith point, respectively.

The relationship between the tortuosity and porosity and average pore diameter of porous materials can be determined by Eqs. (8) and (9), but the process of calculating tortuosity is still complicated. A continuous pore with a tortuosity effect is described by the tortuosity factor (τ), which is the ratio of the tortuosity (ζ) to the limited length (f), i.e., $\tau=\zeta/f$. The results of the tortuosity factor are often influenced by the MIP test. So, a convenient model proposed by Nakarai *et al*. (2006) is adopted in this study. The tortuosity factor is defined as a function of porosity:

$$\tau = -1.5\tanh[8.0(\phi_{\text{paste}} - 0.25)] + 2.5, \qquad (10)$$

where ϕ_{paste} is the effective porosity, representing the sum of gel and capillary pores effective as chloride ion transport pathways per unit volume of cement paste, and can be approximately replaced by $V_{\text{T–por}}$.

The relationship between the tortuosity factor and porosity is shown in Fig. 3. With the growth of porosity, the tortuosity factor decreases. When the porosity is above 0.5, the tortuosity factor is close to 1.0. These facts imply that the tortuosity effect of continuous pores on transport properties almost disappears at high porosities.

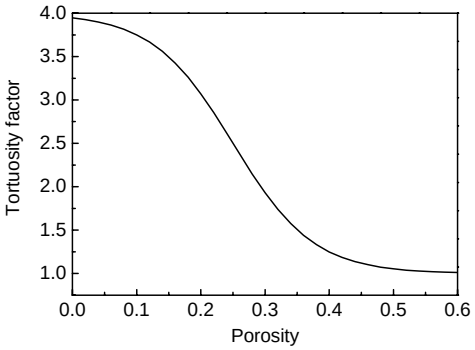

Fig. 3 Effect of porosity on toruosity

Constrictivity is an important parameter for characterizing a continuous pore with an ink-bottle shape. Constrictivity is formulated as an expression of the effect of pore size. Usually, porosity and pore size are taken into account in the study of constrictivity. So pore sizes are thought to be the main determinant of constrictivity. The parameter of constrictivity also adequately considers the interaction between pore structure and ion transport. If the cross-section of a pore space segment is straight, then constrictivity becomes unity, whereas if the segment is restricted at a certain point, the value of constrictivity is less than unity. According to the pore characteristics of cement paste, the constrictivity of pores is defined with respect to the peak pore diameter (Nakarai *et al.*, 2006):

$$\delta = 0.395\tanh[4(\lg r_{\text{cp}}^{\text{peak}} + 6.2)] + 0.405, \qquad (11)$$

where $r_{\text{cp}}^{\text{peak}}$ is the peak radius of capillary pores (m).

The relationship between δ and $r_{\text{cp}}^{\text{peak}}$ is shown in Fig. 4. The value of constrictivity is about 0.8 for ordinary porous materials. However, the pores in cement paste are widely distributed over the nanometer-to-micron scale and pores with variable sizes are randomly connected, while the peak radius of capillary pores ranges from 20 to 120 nm for mature concrete (Maekawa *et al.*, 2003). Thus, the value of constrictivity is of the order of about 0.01 for fine pores in sound cement paste. Of course, it becomes larger for deteriorated cement paste.

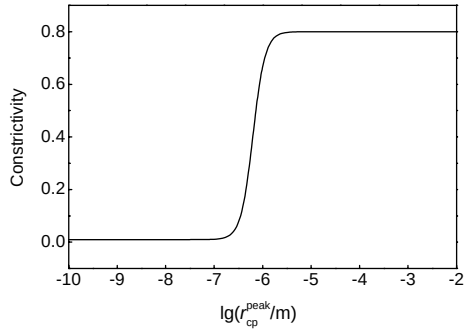

Fig. 4 Effect of peak radius of capillary pores on constrictivity

Based on above analysis, only if the ratio of *w*/*c*, the degree of hydration, and the peak radius of capillary pores are determined, can the development process of pore structures be simultaneously obtained. So Eqs. (6), (10), and (11) are substituted into Eq. (2) to obtain the chloride diffusivity of hardened cement paste in a saturated state.

4 Application of the model in hardened cement paste

To validate the proposed model in the present study, the parameters required by the model were

determined for various mixtures. The experimental details were as follows.

4.1 Experimental materials

Cement paste specimens were prepared using Portland cement type I, which is produced by mixing pure cement clinker with 5% (w/w) of gypsum. The chemical and mineral compositions of the cement are listed in Tables 1 and 2. The *w*/*c* ratios of the cement paste specimens were 0.23, 0.35, and 0.53.

Table 1 Chemical composition of the cement

Oxide	Composition (%, w/w)	Oxide	Composition (%, w/w)
CaO	62.40	TiO_2	0.27
SiO_2	21.38	SO_3	2.25
Al_2O_3	4.67	P_2O_5	0.10
Fe_2O_3	3.31	BaO	0.04
MgO	3.08	ZnO	0.06
K_2O	0.54	MnO	0.18
Na_2O	0.21	LOI	0.95

LOI: Loss on ignition

Table 2 Mineral composition of the cement

Mineral	Composition (%, w/w)	Mineral	Composition (%, w/w)
C_3S	55.5	C_3A	6.5
C_2S	19.1	C_4AF	10.1

4.2 Microcosmic sample preparation and curing

All cement paste samples were mixed with de-aired distilled water, with 1 min of mixing at low speed, and then 2 min at high speed. The pastes were poured into 500 ml plastic beakers, which were vibrated for about 3 min to remove bubbles. Finally, the pastes were poured into PVC tubes with a diameter of 14 mm and vibrated again for 2 min to reduce experimental error. The samples were placed in a room at a temperature of 20 °C for 24 h and then moved to a standard curing room (temperature of 20±3 °C, relative humidity above 95 %). After three days of curing, the samples were removed and split into several parts. The middle part of each sample with a thickness of about 16 mm was selected for testing. Finally, the samples were taken out for measurement of their degree of hydration and porosity at the required standard age. Before testing, the samples were immersed in ethanol to stop further cement hydration by removal of the free water.

4.3 Testing for pore structure

Mercury intrusion measurements were performed with a Micrometrics AutoPore IV 9500 (American Michael Instruments Corp., USA), with a maximum pressure of up to 415 MPa, which determined pore sizes in the range of 3 nm to 360 μm. Measurements were conducted in two stages: a manual low pressure run from 0.003 to 0.21 MPa, and an automated high pressure run from 0.21 to 242 MPa. Data were collected and handled by a computer acting as a control module. After low-pressure testing, the penetrometer was removed and weighed. High-pressure testing was then initiated. The machine was set to equilibrate for 30 s at a contact angle of 130°.

4.4 Testing for degree of hydration

The samples were crushed and ground into powder in an agate pot containing iso-propyl alcohol. Then the powder was sieved using a 0.08 mm sieve. Next the sieved powder was placed in dried and weighed porcelain crucibles and dried at 105 °C for 24 h. The samples were then transferred to a desiccator for 30 min, after which, each sample of 1 g was weighed and the mass denoted as m_0. Finally, the dried samples were placed in a 1050 °C furnace for 3 h and cooled in a desiccator and weighed again, with the mass denoted as $m_{1050\ ^\circ C}$. For each paste, three samples were tested, and the results were averaged. The degree of hydration was determined by the non-evaporable water content:

$$W_n = \frac{L - L_c}{1 - L_c}, \tag{12}$$

where the ignition loss $L=(m_0-m_{1050\ ^\circ C})/m_0$, and L_c is the ignition loss of raw materials.

According to Powers' model (Powers, 1962), the formula for cement hydration can be expressed as

$$\alpha = \frac{100 \times W_n}{0.23}, \tag{13}$$

where α is the cement hydration (%).

4.5 Rapid chloride migration test

Based on the Nernst-Einstein equation and the specimens saturated with concentrated salt method,

the chloride diffusivity of specimens could be rapidly measured (Lu, 1997). The cylinder specimens with 100 mm diameter and 200 mm length were cast and cured in a standard curing room for 28 days. Before testing, a 50-mm-thick slice was taken from the center part of the cylinder specimen. The specimens (ϕ100 mm×50 mm) were saturated with water under vacuum conditions for 24 h, and were then placed in rubber tubes inclined at an angle of 45° in diffusion cells for testing. A solution of 0.2 mol/L KOH was placed inside the rubber tube, and the exterior of the tube was immersed in 5 % (w/w) NaCl+0.2 mol/L KOH solution. The solution surfaces inside and outside the rubber tube were at the same level. A direct current potential of 40 V was applied in two diffusion cells during each test; the duration of testing could be estimated from the initial current, which was measured from the electric circuit at the beginning of the test. According to the penetration depth of chloride ions, the diffusivity of specimens can be calculated using the following equation:

$$D_{\mathrm{RCM},0} = 2.872\times10^{-6}[Th(x_{\mathrm{d}} - \alpha\sqrt{x_{\mathrm{d}}})/t], \quad (14)$$

where $D_{\mathrm{RCM},0}$ is the migration diffusion coefficient (m^2/s), x_{d} is the penetration depth of chloride ions (m), t is the test duration, h is the height of the specimen (m), T is the temperature (K), and $\alpha = 3.338\times10^{-3}\sqrt{Th}$.

5 Results and discussion

It is important to check that cement hydration does not continue during diffusion testing. Thus, after curing, the degree of hydration of each sample was determined. This ensured that the microstructure of the studied specimens remained unchanged during the diffusion tests. The degree of hydration of hardened cement pastes with *w*/*c* ratios of 0.23, 0.35, and 0.53 were 0.573, 0.734, and 0.861, respectively, and the corresponding pore size distributions are shown in Fig. 5. There were two kinds of pore systems in the hardened cement paste. The first peak is the critical pore diameter of capillary pores, usually in the range of 0.01 to 10 μm (Cook and Hover, 1999), while the second peak is the critical pore diameter of gel pores, and its value is less than 0.01 μm. With increasing *w*/*c* ratios, the critical pore diameter of capillary pores becomes larger; i.e., the critical pore diameters of the capillary pores in Fig. 5 are 53, 62, and 77 nm corresponding to the cement pastes with *w*/*c* ratios of 0.23, 0.35, and 0.53. The degree of hydration and critical pore diameter of each material are substituted into Eqs. (6), (10), (11), and (2) to give a predictive chloride ion diffusion coefficient, once they are determined. The predicted results were compared with the results of rapid chloride migration testing (Table 3). The predicted values were almost in accordance with the experimental results.

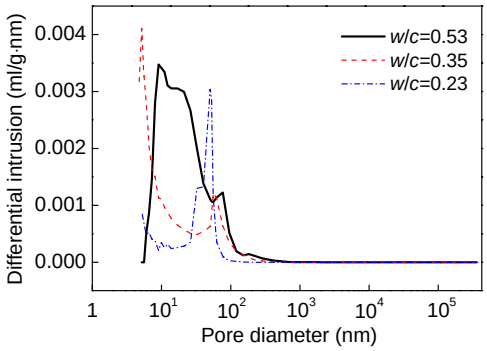

Fig. 5 Pore size distribution of hardened cement paste

Note that in the original constrictivity model (Ishida *et al.*, 2009; Maekawa *et al.*, 2009), the peak radius of the capillary pores in Eq. (11) does not correspond to that measured by the MIP test, but relates to computed pore parameters. However, the small differences between estimates of the peak radius of capillary pores from the computed model and the MIP test have little influence on the calculated results of constrictivity. To facilitate the calculation in practice, in our study the computed peak radius of the capillary pores is replaced approximately by that obtained by MIP.

To further validate the model, we considered published data (Ngala and Page, 1997; Caré, 2003; Oh and Jang, 2004; Huang *et al.*, 2010). The chloride ion diffusion coefficient, degree of hydration of the cement, and critical pore size of capillary pores were given by Caré (2003). The chloride ion diffusion coefficients of cement paste at different curing ages were determined by Oh and Jang (2004), while the chloride ion diffusion coefficients of cement paste at different curing ages and different *w*/*c* ratios were

measured by Negala and Page (1997) and Huang *et al.* (2010). Since the degree of hydration of cement was not given by some authors, for prediction consistency, the relationship between the degree of hydration and *w*/*c* ratio and curing age can be expressed as $\alpha=0.716t^{0.0901}\exp[-0.103t^{0.0719}/(w/c)]$. Another important parameter, constrictivity, needs to be calculated. Fig. 6 shows a comparison of the computed distributions of porosity for different mature mortars with different *w*/*c* ratios and different degrees of hydration (Maekawa *et al.*, 2003; 2009). The peaks of capillary pore calculated by the original model are at about 150 and 300 nm for mortars of *w*/*c*=0.45 and *w*/*c*=0.65, respectively. Therefore, when the *w*/*c* ratio is above 0.5, the peak radius of capillary pores in the references (Ngala and Page, 1997; Caré, 2003; Oh and Jang, 2004; Huang *et al.*, 2010) can be considered to be approximately 260 nm in this study.

The predicted results and experimental data reported in the references (Ngala and Page, 1997; Caré, 2003; Oh and Jang, 2004; Huang *et al.*, 2010) are listed in Table 3. The results predicted by our proposed model are in agreement with those reported in the literature. Of course, due to the limitation of experimental conditions and differences between specimens studied by different researchers, there is some error between the predicted and experimental results, but the error can be accepted theoretically.

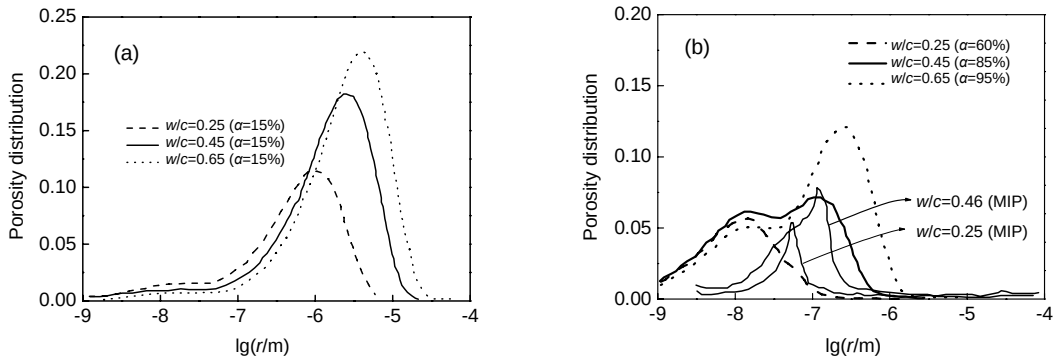

Fig. 6 Comparison of computed microstructures for different mortars (Maekawa *et al.*, 2003; 2009)

(a) Young mortar; (b) Seven day cured mature mortar. *r*: pore radius. Curves of *w*/*c* (0.25 and 0.46, MIP) are obtained by mercury intrusion porosimetry (MIP) measurements

Table 3 Comparison of predicted and experimental results

Research	*w*/*c*	Total porosity (%)	Tortuosity factor	Constrictivity	D_p ($\times10^{-12}$ m^2/s)		Ratio*
					Predicted	Experimental	
Ours	0.23	0.24	2.61	0.010	0.73	1.03	1.43
	0.35	0.37	1.61	0.010	2.66	3.26	1.23
	0.53	0.45	1.12	0.010	7.41	10.70	1.44
Caré (2003)	0.45	0.41	1.23	0.010	5.46	5.65	1.04
Oh and Jang (2004)	0.35	0.35	1.48	0.010	3.29	3.76	1.14
	0.45	0.43	1.17	0.010	6.30	6.56	1.04
	0.55	0.48	1.07	0.013	11.01	15.70	1.43
Ngala and Page (1997)	0.40	0.38	1.33	0.010	4.37	4.28	0.98
	0.50	0.45	1.13	0.010	7.13	8.43	1.18
	0.60	0.50	1.06	0.013	12.03	13.10	1.09
	0.70	0.54	1.03	0.015	16.01	21.10	1.32
Huang *et al.* (2010)	0.40	0.39	1.28	0.010	4.83	5.42	1.12
	0.50	0.46	1.11	0.010	7.57	8.24	1.09
	0.60	0.51	1.05	0.013	12.10	13.60	1.12

* Ratio of the experimental result to predicted one of D_p. D_p: effective diffusivity of a porous material

6 Conclusions

1. The model of the relationship between the effective diffusivity of porous materials and pore structure characteristics was further extended, and adopted for predicting chloride diffusivity in hardened cement paste.

2. The model proposed in this paper considered not only the effect of the capillary and gel pores, but also took into account the effect of the tortuosity factor of pores and pore size distribution on chloride diffusivity. The predicted results of the diffusion coefficient of chloride ions were in good agreement with our experimental results, and were almost in accordance with published results.

3. The effective diffusion coefficient of chloride ions could be deduced from Eqs. (6), (10), (11), and (2). As long as the water to cement ratio and the degree of hydration of hardened cement paste were obtained, its pore structure parameters were also determined.

References

AutoPore IV 9500, 2001. Operator's Manual V1.04 Appendix D. Micromeritices Instrument Corporation, USA.

Caré, S., 2003. Influence of aggregates on chloride diffusion coefficient into mortar. *Cement and Concrete Research*, **33**(7):1021-1028. [doi:10.1016/S0008-8846(03)00009-7]

Cook, R.A., Hover, K.C., 1999. Mercury porosimetry of hardened cement pastes. *Cement and Concrete Research*, **29**(6):933-943. [doi:10.1016/S0008-8846(99)00083-6]

Garboczi, E.J., Bentz, D.P., 1992. Computer simulation of the diffusivity of cement-based materials. *Journal of Materials Science*, **27**(8):2083-2092.

Halamickova, P., Detwiler, R.J., Bentz, D.P., 1995. Water permeability and chloride ion diffusion in Portland cement mortars: relationship to sand content and critical pore diameter. *Cement and Concrete Research*, **25**(4):790-802. [doi:10.1016/0008-8846(95)00069-O]

Huang, X.F., Zheng, J.J., Zhou, X.Z., 2010. Simple analytical solution for the chloride diffusivity of cement paste. *Science and Technology of Overseas Building Materials*, **31**(2):4-6 (in Chinese).

Ishida, T., Miyahara, S., Maruya, T., 2008. Chloride binding capacity of mortars made with various Portland cement and mineral admixtures. *Journal of Advanced Concrete Technology*, **6**(2):287-301. [doi:10.3151/jact.6.287]

Ishida, T., Iqbal, P.O., Anh, H.T.L., 2009. Modeling of chloride diffusivity coupled with non-linear binding capacity in sound and cracked concrete. *Cement and Concrete Research*, **39**(10):913-923. [doi:10.1016/j.cemconres.2009.07.014]

Lu, X.Y., 1997. Application of the Nernst-Einstein equation to concrete. *Cement and Concrete Research*, **27**(2):293-302. [doi:10.1016/S0008-8846(96)00200-1]

Maekawa, K., Ishida, T., Kishi, T., 2003. Multi-scale modeling of concrete performance integrated material and structural mechanics. *Journal of Advanced Concrete Technology*, **1**(2):91-126. [doi:10.3151/jact.1.91]

Maekawa, K., Ishida, T., Kishi, T., 2009. Multi-Scale Modeling of Structural Concrete. Taylor & Francis, London and New York, p.118-121.

Mindess, S., Young, F.J, Darwin, D, 2002. Concrete, 2nd Edition. Prentice Hall, USA, p.478-479.

Nakarai, K., Ishida, T., Maekawa, K., 2006. Multi-scale physiochemical modeling of soil-cementitious material interaction. *Soils and Foundations*, **46**(5):653-664. [doi:10.3208/sandf.46.653]

Ngala, V.T., Page, C.L., 1997. Effects of carbonation on pore structure and diffusional properties of hydrated cement pastes. *Cement and Concrete Research*, **27**(7):995-1007.

Oh, B.H., Jang, S.Y., 2004. Prediction of diffusivity of concrete based on simple analytic equations. *Cement and Concrete Research*, **34**(3):463-480. [doi:10.1016/j.cemconres.2003.08.026]

Pivonka, P., Hellmich, C., Smith, D., 2004. Microscopic effects on chloride diffusivity of cement pastes—a scale-transition analysis. *Cement and Concrete Research*, **34**(12):2251-2260. [doi:10.1016/j.cemconres.2004.04.010]

Powers, T.C., 1962. Physical Properties of Cement Paste. Proceedings of the Fourth International Conference on the Chemistry of Cement, Washington, DC. US National Bureau of Standards Monograph, **43**(2):577-613.

Zhang, W.M., Ba, H.J., 2010. Effect of mineral admixtures and repeated loading on chloride migration through concrete. *Journal of Zhejiang University-SCIENCE A (Applied Physics & Engineering)*, **11**(9):683-690. [doi:10.1631/jzus.A0900609]

Zhang, J.Z., Wang, J.Z., Kong, D.Y., 2010. Chloride diffusivity analysis of existing concrete based on Fick's second law. *Journal of Wuhan University of Technology-Materials Science Edition*, **25**(1):142-146. [doi:10.1007/s11595-010-1142-4]